

# Criticality and Superfluidity in Liquid $^4\text{He}$ Under Nonequilibrium Conditions

<sup>1</sup>Peter B. Weichman, <sup>2</sup>Alexa W. Harter, and <sup>2</sup>David L. Goodstein

<sup>1</sup>*Blackhawk Geometrics, 301 Commercial Road, Suite B, Golden, CO 80401*

<sup>2</sup>*Condensed Matter Physics 114-36, California Institute of Technology, Pasadena, CA 91125*

We review a striking array of recent experiments, and their theoretical interpretations, on the superfluid transition in  $^4\text{He}$  in the presence of a heat flux,  $Q$ . We define and evaluate a new set of critical point exponents. The statics and dynamics of the superfluid-normal interface are discussed, with special attention to the role of gravity. If  $Q$  is in the same direction as gravity, a self-organized state can arise, in which the entire sample has a uniform reduced temperature, on either the normal or superfluid side of the transition. Finally, we review recent theory and experiment regarding the heat capacity at constant  $Q$ . The excitement that surrounds this field arises from the fact that advanced thermometry and the future availability of a microgravity experimental platform aboard the International Space Station will soon open to experimental exploration decades of reduced temperature that were previously inaccessible.

## CONTENTS

I. Introduction	1
II. Nonequilibrium critical phenomena and scaling	2
A. Superfluid counterflow	2
B. Thermodynamic formalism	2
C. Nonequilibrium scaling	3
III. The nonequilibrium superfluid-normal interface	6
A. Interface statics	6
B. Transition from thermodynamic to interface state	7
C. Interface dynamics	8
IV. The self-organized critical state	10
V. Specific heat at constant heat current	11
A. Enhanced specific heat	11
B. The superfluid breakdown temperature	12
C. Experimental measurements	12
VI. Conclusions	15
References	15

## I. INTRODUCTION

Due to its extraordinary purity and insensitivity to external perturbations, superfluid  $^4\text{He}$  has long been the best system for accurate, detailed experimental investigations of phase transitions and critical phenomena. The essence of superfluidity, however, lies in the dynamics of flowing helium, rather than in equilibrium properties such as the specific heat and the superfluid density. In recent years, considerable experimental attention has been focused on the behavior of liquid helium, near the lambda transition temperature,  $T_\lambda$ , when a flux of heat,  $Q$ , is passed through it (Duncan *et al.*, 1988; Liu and Ahlers, 1996; Moeur *et al.*, 1997; Day *et al.*, 1998; Harter *et al.*, 2000). This article reviews the wealth of exciting new physical phenomena uncovered by these experiments and by the parallel theoretical investigations (Onuki, 1983; Haussmann and Dohm, 1992a; Haussmann

and Dohm, 1994; Weichman *et al.*, 1998; Haussmann, 1999a; Weichman and Miller, 2000).

At sufficiently small  $Q$ , superfluid  $^4\text{He}$  transports heat essentially without dissipation, by means of superfluid-normal fluid counterflow. At higher  $Q$ , or as  $T$  approaches  $T_\lambda$ , this transport mode breaks down. In Sec. II we discuss the phase diagram of helium in the  $Q$ - $T$  plane. In this plane, the superfluid state is bounded by a transition curve,  $Q_c(T)$ , outside of which dissipative flow takes over. We also introduce and evaluate a new set of critical exponents that arise as a consequence of superflow.

In Sec. III we describe an inhomogeneous phase where the heat flows through both normal and superfluid regions, separated by an interface region that is neither normal nor superfluid. In the normal region the heat flux produces a static temperature gradient. In the superfluid region, the heat flows at constant temperature. In the interface region, a transition between these types of behavior is mediated by fluctuations in a way that is not yet accessible either to experiment or to theory.

A recurring theme throughout the article is the fundamental limitation imposed by the Earth's acceleration due to gravity,  $g_e$ , on the resolution of Earth-based experiments. Gravity produces a pressure gradient across the sample, leading to a variation in the local lambda transition temperature  $T_\lambda(z)$  with height  $z$  according to

$$\partial_z T_\lambda(z) = -\gamma \frac{g}{g_e}, \quad \gamma \simeq 1.27 \frac{\mu\text{K}}{\text{cm}}. \quad (1.1)$$

For generality, the possibility of gravity  $g$  different from that on Earth is included. For  $g = g_e$  the transition temperature therefore decreases by  $1.27\mu\text{K}$  per centimeter of column height. If  $T$  is tuned so that, say, the center of the cell is at the local lambda point, the upper region will be superfluid while the lower region will be normal fluid.

The interface between, defined as the region over which the local properties differ significantly from those of a bulk system at the same local temperature and pressure, is about 0.1 mm wide on Earth (Muzikar and Giordano, 1989). This figure also estimates the maximum possible critical correlation length in the system.

The inhomogeneity induced by  $g_e$  causes the critical singularities to be rounded on a scale set by the height of the cell. Balancing gravity effects against finite size effects, which enter if the cell is too small, the optimal cell height is about 0.3 mm, leading to rounding on a scale  $\epsilon \equiv (T - T_\lambda)/T_\lambda \sim 10^{-7}$ . Present thermometry (Lipa *et al.*, 1996; Day *et al.*, 1998) is capable of resolving reduced temperatures  $\epsilon$  that are 3–4 orders of magnitude smaller than this. In essence there is a new frontier, consisting of decades of previously unavailable reduced temperature around  $T_\lambda$ , that can only be explored in microgravity. Experiments measuring equilibrium specific heat (Lambda Point Experiment—LPE) (Lipa *et al.*, 1996) and finite size effects (Confined Helium Experiment—CHEX) have recently flown aboard the space shuttle.

Gravity also has a strong effect on the interface region discussed in Sec. III. As we have seen above, the interface is compressed by gravity to a width of about 0.1 mm, too small to be studied experimentally. The interface region will be studied in an experiment (Critical Dynamics Experiment—DYNAMX) presently being prepared for a low temperature microgravity platform (Low Temperature Microgravity Physics Facility—LTMPF) that is to be part of the International Space Station (ISS).

Although gravity is detrimental to some measurements, there can also be interesting new physics when both gravity and heat current are present. In Sec. IV we describe the so-called *self-organized critical* (SOC) state, in which  $g$  and  $Q$  conspire to produce a new, essentially homogeneous, nonequilibrium state where the temperature  $T(z)$  precisely parallels  $T_\lambda(z)$  at a fixed  $Q$ -dependent distance. At larger  $Q$ , this state undergoes a transition from normal to superfluid, with the temperature gradient supported by a stream of vortices in the latter.

Finally, in Sec. V we discuss the specific heats under heat flow, predicted (Haussmann and Dohm, 1994; Chui *et al.*, 1996; Haussmann and Dohm, 1996), and subsequently confirmed (Harter *et al.*, 2000), to be *enhanced* above the equilibrium form, with a singularity predicted at the phase boundary  $Q_c(T)$ . This experiment too ultimately needs to be performed at very low  $Q$ , and the required microgravity version is currently being proposed.

## II. NONEQUILIBRIUM CRITICAL PHENOMENA AND SCALING

We begin by presenting the basic mathematical background within which the physical phenomena we discuss in later sections is most clearly described and understood.

The language of phase transitions and critical phenomena, under both equilibrium and nonequilibrium conditions, is that of critical exponents, scaling relations, and scaling functions, which quantify the scale invariant nature of a system near its critical point. In order to keep the discussion at as elementary a level as possible, we will introduce the theory in close analogy to that appropriate to equilibrium classical magnetic and liquid-vapor critical points. The near-dissipationless nature of superflow in  $^4\text{He}$  makes this analogy especially fruitful in describing nonequilibrium superfluidity.

### A. Superfluid counterflow

Under conditions where a uniform heat flux  $\mathbf{Q}$  is applied to superfluid  $^4\text{He}$ , a thermal counterflow is created in which the normal fluid moves along with  $\mathbf{Q}$  at velocity  $\mathbf{u}_n$ , and the superfluid moves oppositely with velocity  $\mathbf{u}_s$ . For sufficiently small heat current not too close to  $T_\lambda$  [more precisely, one requires  $Q < Q_c(T)$ , with  $Q_c(T)$  defined in Fig. 2 and (2.20) below] the temperature  $T < T_\lambda$  is essentially uniform and the heat flux is

$$\mathbf{Q} = TS\rho\mathbf{u}_n, \quad (2.1)$$

where  $S$  is the entropy per unit mass,  $\rho = \rho_s + \rho_n$  is the total mass density, composed of superfluid and normal fluid parts, and  $\mathbf{u}_n$  is the normal fluid velocity. Since there is no net mass flow, one has  $\mathbf{j}_n = -\mathbf{j}_s$ , where  $\mathbf{j}_s = \rho_s\mathbf{u}_s$  and  $\mathbf{j}_n = \rho_n\mathbf{u}_n$  are, respectively, the superfluid and normal fluid mass current densities, and  $\mathbf{u}_s$  is the superfluid velocity. Close to  $T_\lambda$  one finds experimentally  $S \simeq S_\lambda \equiv 1.58\text{J/gK}$ ,  $\rho_s \approx \rho_0|\epsilon|^\zeta$ , with  $\rho_0 \simeq 0.37\text{g/cm}^3$ , critical exponent  $\zeta \simeq 0.671$ , and  $\rho_n \simeq \rho \simeq 0.14\text{g/cm}^3$ . Thus, in experimentally motivated units,

$$u_s \approx 7.9 \times 10^{-3} \frac{Q}{1\mu\text{W/cm}^2} \left( \frac{10^{-6}}{|\epsilon|} \right)^\zeta \text{ cm/s} \quad (2.2)$$

$$u_n \approx 2.1 \times 10^{-6} \frac{Q}{1\mu\text{W/cm}^2} \text{ cm/s}. \quad (2.3)$$

At experimentally accessible values  $Q = 1\mu\text{W/cm}^2$  and  $|\epsilon| = 10^{-6}$ ,  $u_s$  is a modest 80  $\mu\text{m/s}$  and  $u_n$  is nearly four orders of magnitude smaller.

### B. Thermodynamic formalism

The isothermal condition allows an effective thermodynamic description of the finite  $\mathbf{Q}$  state (Hohenberg and Martin, 1965). Although nonequilibrium scaling does not rely on this, a more intuitive description of a number of phenomena special to superfluidity results, and so it is worthwhile presenting the theory in this context.

In the frame of reference moving with the normal fluid (in which there is no heat flow), the differential of the free energy density  $F(T, \mathbf{U}_s)$  may be written,

$$dF = -SdT + \mathbf{J}_s \cdot d\mathbf{U}_s, \quad (2.4)$$

in which  $\mathbf{U}_s = \mathbf{u}_s - \mathbf{u}_n$  and

$$\mathbf{J}_s = \left( \frac{\partial F}{\partial \mathbf{U}_s} \right)_T = \rho_s \mathbf{U}_s, \quad (2.5)$$

with the second equality serving as a *definition* of  $\rho_s(T, U_s)$  when  $U_s$  is not small. Near  $T_\lambda$  the smallness of  $\mathbf{u}_n$  implies that  $\mathbf{U}_s \simeq \mathbf{u}_s$  and  $\mathbf{J}_s \simeq \mathbf{j}_s$ . In this frame one has the defining relation  $\mathbf{U}_s = (\hbar/m)\nabla\phi$ , where  $m$  is the  $^4\text{He}$  atomic mass, and

$$\phi(\mathbf{r}) = \frac{m}{\hbar} \mathbf{U}_s \cdot \mathbf{r} \quad (2.6)$$

is the phase of the superfluid order parameter  $\psi = |\psi|e^{i\phi}$ . Thus,  $\psi$  rotates in the complex plane as one moves along the direction  $\mathbf{U}_s$ , generating a kind of helical structure. The effective thermodynamic description (2.4) relies on the existence of a time-independent  $\psi$  in the presence of a finite phase gradient. In fact, thermally nucleated phase slips in the helical structure (interpreted as tunneling between different metastable local minima of the free energy) lead to small temperature gradients and decay of superflow. However, the decay time is extremely large at low heat currents and temperatures not too close to  $T_\lambda$  (Langer and Fisher, 1967). The thermodynamic description (2.4) is valid on time scales smaller than this. As  $\mathbf{U}_s$  increases, both the order parameter magnitude  $|\psi(U_s, T)|$  and the superfluid density are suppressed relative to their equilibrium values at  $U_s = 0$ ,  $Q = 0$ .

Variations at constant  $\mathbf{Q} = -TS\mathbf{J}_s$  are most conveniently performed by defining the Legendre transformed free energy  $\Phi(T, \mathbf{J}_s) = F - \mathbf{J}_s \cdot \mathbf{U}_s$  with differential

$$d\Phi = -SdT - \mathbf{U}_s \cdot d\mathbf{J}_s. \quad (2.7)$$

Close to  $T_\lambda$ , where  $TS \simeq T_\lambda S_\lambda$  is essentially constant, variations at constant  $\mathbf{Q}$  are asymptotically the same as those at constant  $\mathbf{J}_s$ . For example, the specific heat at fixed  $\mathbf{Q}$  may be taken as

$$C_Q = T \left( \frac{\partial S}{\partial T} \right)_{\mathbf{J}_s}, \quad (2.8)$$

where  $S(T, \mathbf{J}_s) = -(\partial\Phi/\partial T)_{\mathbf{J}_s}$ . With the above observation in mind, we shall henceforth treat  $\mathbf{J}_s$  and  $\mathbf{Q}$  as differing only by a constant factor.

### C. Nonequilibrium scaling

The fact that  $\mathbf{U}_s$  and  $\mathbf{J}_s$  (or  $\mathbf{Q}$ ) may be treated as thermodynamically conjugate variables has important consequences for the structure of the thermodynamic functions

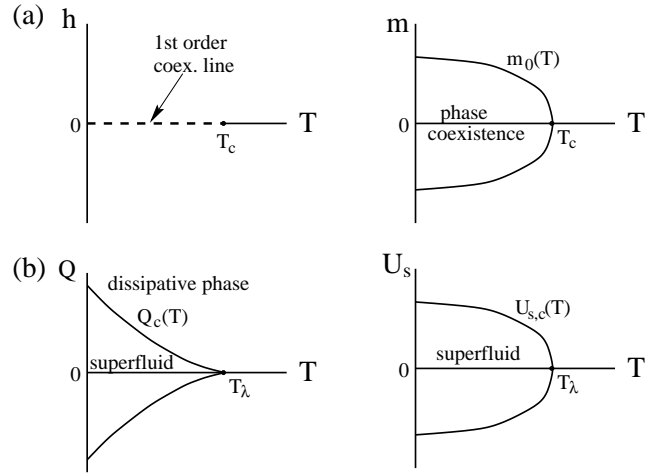


FIG. 1. Comparison of phase diagrams in (a) conventional  $T$ - $h$  and  $T$ - $m$  spaces and (b) superfluid  $T$ - $Q$  and  $T$ - $U_s$  spaces. Here,  $m_0(T)$  is the spontaneous magnetization, or the liquid density minus the critical density. The critical lines  $Q_c(T)$  and  $U_{s,c}(T)$ , enclose the region of stable superflow, which corresponds also to the region of validity of the thermodynamic description, and like the thermodynamic description itself are sharp only in the absence of phase slips. The different shapes of these curves near  $T_\lambda$  are determined by the fact that  $\Delta_Q > 1$ , while  $\beta_Q < 1$  [see equations (2.18)–(2.21) below]. The nature of the critical behavior as  $Q$  approaches  $Q_c$  from below, and the nature of the inhomogeneous dissipative phase for  $Q > Q_c$ , will be discussed in later sections. A major difference between (a) and (b) is the lack of a first order line below  $T_\lambda$  in the latter. Thus,  $h$  vanishes throughout the phase coexistence region in the  $T$ - $m$  plane, whereas  $Q \propto J_s = \rho_s U_s$  varies continuously throughout the superfluid phase in the  $T$ - $U_s$  plane.

near  $T_\lambda$  (Fisher, 1973). We proceed by analogy with the conjugate variables  $h$  and  $m$  at conventional critical points, where  $h$  is the external magnetic field and  $m$  the magnetization at a Curie point, or  $h$  is the difference from critical pressure and  $m$  the difference from critical density at a liquid-vapor critical point. There the free energy  $A(T, h)$ , analogous to  $\Phi$ , has differential  $dA = -SdT - mdh$  and its singular part  $A_s$  obeys an *asymptotic scaling form* [see, e.g., (Fisher, 1983)],

$$A_s(T, h) = E_0 |\epsilon|^{2-\alpha} \mathcal{A} \left( \frac{D_0 h}{|\epsilon|^\Delta} \right), \quad (2.9)$$

in which  $\alpha$  is the specific heat exponent,  $\Delta$  is the “gap exponent,”  $\mathcal{A}(x)$  is a universal scaling function, and  $E_0$ ,  $D_0$  are nonuniversal scale factors, specified uniquely via, say, the normalizations  $\mathcal{A}(0) = \mathcal{A}'(0) = 1$ . There are actually two scaling functions,  $\mathcal{A}_\pm(x)$  for  $\pm\epsilon > 0$ , but we shall primarily be interested in the ordered phase  $\epsilon < 0$  and consider only  $\mathcal{A}_- \equiv \mathcal{A}$ .

Similarly, the singular part of the superfluid free energy,  $\Phi_s$ , is expected to obey the scaling form,

$$\Phi_s(T, Q) = A_0 |\epsilon|^{2-\alpha} Y \left( \frac{Q}{Q_0 |\epsilon|^{\Delta_Q}} \right), \quad (2.10)$$

in which  $\alpha \simeq -0.013$  (Lipa *et al.*, 1996) is again the usual equilibrium specific heat exponent,  $\Delta_Q$  is the gap exponent for  $Q$ ,  $Y(y)$  is the  $\epsilon < 0$  universal scaling function, and  $A_0, Q_0$  are nonuniversal scale factors, specified uniquely via, say, the normalizations  $Y(0) = Y''(0) = 1$  [ $Y(y)$  must be an even function of  $y$  due to the obvious symmetry under sign reversal of  $Q$ ].

The derivative of (2.9) with respect to  $h$  yields

$$m(T, h) = -E_0 D_0 |\epsilon|^\beta \mathcal{A}' \left( \frac{D_0 h}{|\epsilon|^\Delta} \right) \quad (2.11)$$

where the prime denotes derivative with respect to argument and the order parameter exponent  $\beta$  obeys the scaling relation  $\beta = 2 - \alpha - \Delta$ . The second  $h$  derivative yields the order parameter susceptibility (compressibility, in the case of a liquid-vapor critical point)

$$\chi(T, h) = -E_0 D_0^2 |\epsilon|^{-\gamma} \mathcal{A}'' \left( \frac{D_0 h}{|\epsilon|^\Delta} \right) \quad (2.12)$$

with  $\gamma = \alpha + 2\Delta - 2$ , which then yields the famous Essam-Fisher scaling law  $\alpha + 2\beta + \gamma = 2$  (Fisher, 1983).

Similarly, the derivative of  $\Phi_s$  with respect to  $J_s$  yields  $U_s$  in the form (Haussmann and Dohm, 1992b)

$$U_s(T, Q) = -B_0 |\epsilon|^{\beta_Q} Y' \left( \frac{Q}{Q_0 |\epsilon|^{\Delta_Q}} \right), \quad (2.13)$$

where  $B_0 = A_0 T_\lambda S_\lambda / Q_0$ , and one has the generalized order parameter exponent scaling relation

$$\beta_Q = 2 - \alpha - \Delta_Q. \quad (2.14)$$

The equilibrium superfluid density enters the free energy  $F$  via a term  $\Delta F_s = \frac{1}{2} \rho_s U_s^2$  for small  $U_s$ . The Legendre transform yields a term  $\Delta \Phi_s = -J_s^2 / 2\rho_s$  for small  $J_s$ , and the inverse of the superfluid density now appears in the theory as a generalized susceptibility:

$$\begin{aligned} \frac{1}{\rho_s(T, Q=0)} &= - \left( \frac{\partial^2 \Phi_s}{\partial J_s^2} \right)_{T, J_s=0} = \left( \frac{\partial U_s}{\partial J_s} \right)_{T, J_s=0} \\ &= - \frac{R_0 Y''(0)}{|\epsilon|^{\gamma_Q}} \end{aligned} \quad (2.15)$$

where  $R_0 = A_0 (T_\lambda S_\lambda / Q_0)^2$  and the generalized susceptibility exponent  $\gamma_Q$  obeys the Essam-Fisher relation (Fisher, 1983),

$$\gamma_Q = \zeta = 2\Delta_Q + \alpha - 2 \quad (2.16)$$

$$\alpha + 2\beta_Q + \gamma_Q = 2 \quad (2.17)$$

Generally the gap exponent is independent of  $\alpha$  and must be separately determined. However, in the superfluid problem the Josephson relation [see, e.g., (Pfeuty *et al.*,

1974) and references therein] yields  $\zeta = 2 - \alpha - 2\nu = (d-2)\nu$ . Here  $\xi \approx \xi_0 / |\epsilon|^\nu$  with, in dimension  $d = 3$ ,  $\nu = \zeta \simeq 0.671$  and  $\xi_0 \simeq 3.4 \text{ \AA}$  (Goldner and Ahlers, 1992), describes the divergence of the superfluid coherence length,  $\xi = (m^2 k_B T / \hbar^2 \rho_s)^{1/(d-2)}$ , and the second equality follows from the hyperscaling relation  $2 - \alpha = d\nu$  (Fisher, 1973; Fisher, 1983). We therefore identify

$$\Delta_Q = 2 - \alpha - \nu = (d-1)\nu. \quad (2.18)$$

This scaling law implies that  $Q$  scales with the cross-sectional area  $\xi^{d-1}$  of a correlation volume  $\xi^d$ :  $Q$  becomes significant when the power incident on a correlation area is of order  $Q_0 \xi_0^{d-1}$ .<sup>\*</sup> From (2.14) one obtains

$$\beta_Q = \nu, \quad (2.19)$$

This relation has the interpretation that  $(m/\hbar) \mathbf{U}_s$ , which has dimensions of inverse length, scales with the inverse correlation length  $\xi^{-1}$ : the phase gradient has a significant effect when its wavelength  $2\pi\hbar/mU_s$  becomes comparable to  $\xi$ . Note that, more typically, one begins with the latter assumption and reverses the above argument to *derive* the Josephson relation.

Just as arbitrarily small  $h$  smears the singular behavior near a Curie point, one expects an arbitrarily small  $Q$  to either smear or drastically alter the lambda point critical behavior. This is consistent with  $\Delta_Q > 0$ , implying that the scaling argument  $y$  diverges as  $|\epsilon| \rightarrow 0$  at any finite  $Q$ , serving to define  $Q$  as a *relevant perturbation* to the lambda point (Fisher, 1973). In Fig. 1 a schematic of the expected phase diagram is shown, contrasting it with that for a conventional critical point. The lines  $Q_c(T)$  and  $U_{s,c}(T)$  are the boundaries beyond which superfluidity breaks down: for  $Q > Q_c$ , due to suppression of the order parameter and superfluid density, the heat current is too large for the superfluid to support isothermal heat transport, and a nonequilibrium phase transition to a new dissipative phase occurs. The nature of this phase will be discussed in Sec. III below. In Fig. 2 we sketch the isothermal equations of state for the conventional and superfluid systems. At a fixed subcritical temperature the

---

<sup>\*</sup>One may estimate  $Q_0$  as follows. Two scale factor universality yields a form  $C_s = k_B (R_\xi / \xi)^d / \alpha |\epsilon|^2$  for the singular part of the equilibrium specific heat below  $T_\lambda$ , where the hyperuniversal ratio  $R_\xi \simeq 0.90$  in  $d = 3$  (Hohenberg *et al.*, 1976). This must match the scaling form (2.10) at  $Q = 0$  and determines  $A_0 |\epsilon|^{2-\alpha} = [k_B T_\lambda / \alpha (1 - \alpha) (2 - \alpha)] (R_\xi / \xi)^d$  [with the choice  $Y(0) = 1$ ]. Equating the quadratic terms  $A_0 |\epsilon|^{2-\alpha} (Q / Q_0 |\epsilon|^{\Delta_Q})^2 = -J_s^2 / \rho_s$  [with the choice  $Y''(0) = 1$ ], one obtains finally  $Q_0 = T_\lambda S_\lambda \sqrt{-A_0 \rho_0}$ , and  $Q_0 \xi_0^{d-1} = m k_B T_\lambda^2 S_\lambda R_\xi^{d/2} / \hbar \sqrt{-\alpha(1-\alpha)(2-\alpha)}$  (using  $\rho_0 = m^2 k_B T_\lambda / \hbar^2 \xi_0^{d-2}$ ). Substitution of experimental numbers yields  $A_0 \simeq -21 \text{ J/cm}^3$  and  $Q_0 \simeq 30 \text{ kW/cm}^2$ .

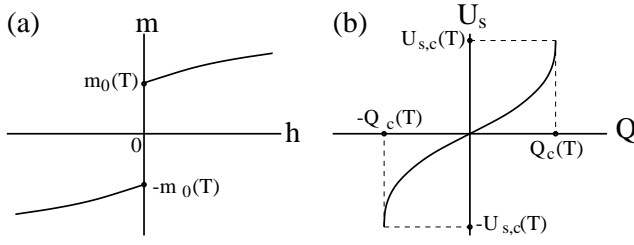


FIG. 2. Comparison of the isothermal equation of state (a) in the conventional  $h$ - $m$  plane and (b) in the superfluid  $Q$ - $U_s$  plane. At  $h = 0$  there is a first order transition between up and down magnetized states, or between liquid and vapor states. As  $|h|$  increases,  $|m(T, h)|$  increases as well. As  $|Q|$  increases  $|U_s|$  increases until the superfluid breaks down at  $|Q| = Q_c(T)$ , at which point  $U_s(Q, T)$  has a square root cusp. At this same point the specific heat at constant  $U_s$  also has a square root cusp (Haussmann and Dohm, 1994), while the specific heat at constant  $Q$  has an inverse square root divergence (Chui *et al.*, 1996).

conventional system displays the usual first order jump in  $m$  at  $h = 0$  between up and down magnetized states, or between liquid and vapor states. The superfluid system displays a continuous variation of  $U_s$  with  $Q$ , but at  $|Q| = Q_c(T)$  encounters the boundary between superfluid and dissipative phases. At this point  $U_s(Q)$  has a square root cusp (Haussmann and Dohm, 1994), corresponding to a strong suppression of  $\rho_s$  and a divergent susceptibility  $(\partial U_s / \partial J_s)_T$ . This singularity is exhibited in the scaling form (2.10) as square root cusps in  $Y(y)$  at some finite value  $y = \pm y_c$ . This yields the predictions

$$Q_c(T) \approx Q_0 y_c |\epsilon|^{\Delta_Q} \quad (2.20)$$

$$U_{s,c}(T) \approx B_0 Y'(y_c) |\epsilon|^{\beta_Q} \propto Q_c(T)^{1/\delta_Q}, \quad (2.21)$$

in which

$$\delta_Q = \Delta_Q / \beta_Q = 1 + \gamma_Q / \beta_Q. \quad (2.22)$$

The latter relation generalizes the Widom scaling law  $m(T_c, h) \propto h^{1/\delta}$  with  $\delta = \Delta/\beta = 1 + \gamma/\beta$  which follows from (2.11) in the limit  $\epsilon \rightarrow 0$  [the asymptotic behavior  $\mathcal{A}'(x) \sim x^{\beta/\Delta}$  as  $x \rightarrow \infty$  is required for consistency] (Fisher, 1983). From (2.16) and (2.19) one obtains explicitly  $\delta_Q = d - 1$ . As will be discussed in Sec. V, the specific heats at constant  $U_s$  and  $Q$  are also singular at  $U_{s,c}(T)$  and  $Q_c(T)$  (Haussmann and Dohm, 1994; Chui *et al.*, 1996; Haussmann and Dohm, 1996).

The coherence length itself obeys a scaling form

$$\xi(T, Q) = \xi_0 |\epsilon|^{-\nu} \Xi \left( \frac{Q}{Q_0 |\epsilon|^{\Delta_Q}} \right), \quad (2.23)$$

with  $\Xi(0) = 1$ . Considering variations of  $\xi$  at a fixed value of  $y = Q/Q_0 |\epsilon|^{\Delta_Q}$ , one may write

$$\xi = \xi_0 (Q/Q_0)^{-\nu_Q} y^{\nu_Q} \Xi(y) \quad (2.24)$$

$$\nu_Q \equiv \nu / \Delta_Q = 1/(d - 1), \quad (2.25)$$

exponent	general $d$	$d = 3$
$\nu$	$1/2 \leq \nu(d) \leq \infty$	0.671
$\alpha$	$2 - d\nu$	-0.013
$\zeta$	$2 - \alpha - 2\nu = (d - 2)\nu$	0.671
$\Delta_Q$	$2 - \alpha - \nu = (d - 1)\nu$	1.342
$\beta_Q$	$\nu$	0.671
$\gamma_Q$	$\zeta$	0.671
$\delta_Q$	$1 + \gamma_Q / \beta_Q = d - 1$	2
$\nu_Q$	$\nu / \Delta_Q = 1/(d - 1)$	1/2

TABLE I. Equilibrium and nonequilibrium critical exponents and their values. Note that no exact expression for the correlation length exponent  $\nu(d)$  is known, aside from the boundary values  $\nu(2) = \infty$  and  $\nu(d \geq 4) = \frac{1}{2}$ , but all other exponents are either given exactly or in terms of  $\nu$ . There are other independent exponents (e.g., the critical correlation exponent  $\eta \simeq 0.02$ ), but they happen not to be involved in any of the experiments we discuss. Expressions in the center column involving  $d$  explicitly require hyperscaling, and are therefore valid only for  $d \leq 4$ . For  $d \geq 4$  the exponents all stick to their mean field values, and may be determined by substituting  $\nu = \frac{1}{2}$ ,  $\alpha = 0$  into the non-explicitly  $d$ -dependent forms of the scaling relations.

serving to define an exponent describing the characteristic variation of  $\xi$  with  $Q$ . Attempts to verify the scaling relations (2.20) and (2.25), with  $\Delta_Q = 2\nu$  and  $\nu_Q = 1/2$  in  $d = 3$ , will be discussed in later sections.

In Table I we summarize the various critical exponents we have defined, along with their values in general dimension  $d$  and in  $d = 3$ .

As a final comment, we note that verifications of certain dynamical scaling laws in  $^4\text{He}$  are complicated by a fundamental problem associated with the existence of very slowly convergent, nonasymptotic dynamic effects. Scaling forms like (2.10) implicitly assume that  $|\epsilon|$  is sufficiently small that all *irrelevant* scaling variables may be ignored. It turns out that a certain *Wegner exponent*  $\omega$  controls the relevance of *mass and heat diffusion* on the dynamic critical behavior (Hohenberg and Halperin, 1977) through an additional scaling variable  $w \equiv \gamma_0 |\epsilon|^\omega$ , where  $\gamma_0$  is a parameter of order unity in the Model F equations (Hohenberg and Halperin, 1977) (describing the near-critical dynamics of  $^4\text{He}$ ) which couples entropy and density fluctuations to order parameter fluctuations.<sup>†</sup> The variable  $w$  does not appear in

<sup>†</sup>The Hohenberg-Halperin Models A–J classify the different dynamical universality classes encountered most commonly in physical systems. The dynamical behavior depends qualitatively, for example, on whether or not the order parameter is a conserved density, and whether or not it is coupled to other conserved densities (like mass or energy). The Model F equations are the simplest possible description of a non-conserved

any equilibrium scaling function (where such fluctuations may be completely “integrated out” of the partition function), but does appear in those involving dissipative transport, e.g., that of the thermal conductivity (Haussmann and Dohm, 1992a). Since  $\omega \simeq 0.008$  (Dohm, 1991) is very small at the superfluid transition this variable vanishes extremely slowly as  $|\epsilon| \rightarrow 0$ :  $\epsilon = 10^{-125}$  leads only to  $|\epsilon|^\omega = 0.1$ . The scaling function then has a very slow parametric dependence on  $w$ , leading to “quasi-scaling” (Haussmann and Dohm, 1992a) of the heat conductivity, and hence to an apparent slow variation of the associated critical exponent with  $w$ . Measured dynamic critical exponents affected in this way may typically be expected to differ from their true asymptotic values by 10-20% (Duncan *et al.*, 1988).

The scaling phenomena considered here, however, are mainly those associated with properties of isothermal superfluids, which though out of equilibrium, are nevertheless argued to behave as equilibrium thermodynamic systems. To the extent that this is true (i.e., to the extent that vortex excitations can be ignored), the Model F equations again produce a thermodynamic-type partition function with entropy/density fluctuations integrated out, and finite  $\mathbf{Q}$  enforced by an imposed uniform helical twist in the order parameter (Haussmann and Dohm, 1994). The scaling variable  $w$  will again not appear, and one expects that quasi-scaling will be absent in (2.10) and from all quantities derived from it, and hence that the exponents in Table I will exhibit experimentally their predicted values. On the other hand, the phase boundaries in Fig. 1(b) are defined by the *onset* of dissipative transport, with divergent fluctuations in the local heat current as they are approached. Such fluctuations lead to vortex creation, decay of superflow, breakdown of the effective equilibrium description, and the reappearance of the variable  $w$ . In some sense  $w$  must control the “fuzziness” of the boundary  $Q_c(T)$ , and an experimental test of the relations (2.20) may exhibit quasi-scaling even if, for  $y$  sufficiently less than  $y_c$ , the scaling function  $Y(y)$  does not. This issue is potentially testable by the specific heat measurements discussed in Sec. V. Unfortunately, as exhibited in Fig. 9 below, present data are constrained to lie sufficiently far below  $Q_c(T)$  that both asymptotic and nonasymptotic forms fit equally well.

---

two-component order parameter (the real and imaginary parts of  $\psi$ ) coupled to heat and mass flow, and are believed to provide an asymptotically exact description of the universal critical dynamics of superfluid  $^4\text{He}$ .

### III. THE NONEQUILIBRIUM SUPERFLUID-NORMAL INTERFACE

#### A. Interface statics

Consider a cylindrical cell with a heat current  $\mathbf{Q}$  driven along its axis, labeled by coordinate  $z$ , in which the upstream endwall,  $z = 0$ , has  $T(0) > T_\lambda$ . In the normal phase heat is transported by thermal conduction, which at sufficiently small  $Q$  is described by the Fourier law

$$Q = -\kappa \partial_z T, \quad (3.1)$$

where  $\kappa(T) \approx \kappa_0 \epsilon^{-\mu}$  is the thermal conductivity, predicted to diverge at  $T_\lambda$ , consistent with its infinite value at all  $T < T_\lambda$ . Experimentally one finds (Dingus, *et al.*, 1986; Tam and Ahlers, 1985; Moeur *et al.*, 1997)  $\kappa_0 \simeq 12 \mu\text{W}/\text{cm}^2$  and  $\mu \simeq 0.44$ . In a very tall cell in which  $T$  varies substantially along its length, one may view (3.1) as locally valid with  $\kappa(z) = \kappa[T(z)]$  so long as  $T(z)$  remains sufficiently far above  $T_\lambda$ . “Sufficiently far above  $T_\lambda$ ” may be quantified by the condition that the temperature drop across a coherence length be much smaller than the deviation from  $T_\lambda$ :

$$\xi |\nabla T| \ll T - T_\lambda \Rightarrow \frac{Q\xi}{\kappa \epsilon T_\lambda} \ll 1. \quad (3.2)$$

Putting in  $^4\text{He}$  parameters, this requires

$$\epsilon \gg 6 \times 10^{-8} \left( \frac{Q}{1 \mu\text{W}/\text{cm}^2} \right)^r, \quad r \equiv \frac{1}{1 + \nu - \mu} \simeq 0.81 \quad (3.3)$$

As  $z$  increases,  $T(z)$  will eventually violate (3.3), and one enters a region of *nonlinear heat transport*. In effect,  $\kappa$  becomes a strong function of  $Q$  in this region. Moreover, as illustrated in Fig. 3, at some position  $z_0$ ,  $T(z_0) = T_\lambda$ , and the system enters the superfluid phase for  $z > z_0$ : a nonequilibrium superfluid–normal fluid interface is generated. Far downstream from this interface,  $T(z)$  levels out at a temperature  $T_\infty(Q)$ , one of the nonequilibrium thermodynamic states discussed in Sec. II above. Correspondingly, the order parameter magnitude  $|\psi(z)|$ , which effectively vanishes for  $z < z_0$ , grows in the interface region and saturates at a value  $|\psi_\infty(Q)|$  for  $z \gg z_0$ .<sup>‡</sup>

The interface is the region over which the mode of heat transport converts from conduction to superfluid counterflow. Its characteristic width  $\xi(Q)$ , through which  $T$

---

<sup>‡</sup>In fact  $T(z)$  continues to decrease slowly with  $z$  in the superfluid phase due to rare phase slip events (Haussmann, 1999a; Haussmann, 1999b), so  $T_\infty(Q)$  and  $|\psi_\infty(Q)|$  are not sharply defined, but we shall not dwell on this complication here.

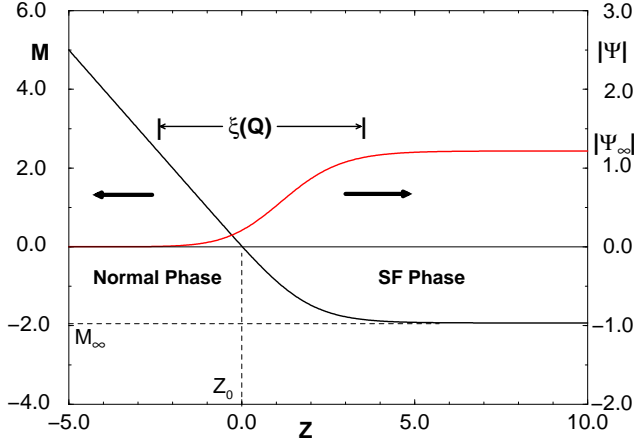


FIG. 3. Scaled temperature and order parameter profiles  $M(Z)$  and  $\Psi(Z)$ , computed within the mean field approximation (Onuki, 1983; Weichman *et al.*, 1998). Here  $Z = z/l(Q)$ ,  $|\Psi| \propto |\psi|l(Q)$  and  $M \propto (T - T_0)l^2(Q)$ , where  $T_0$  is the mean field transition temperature and  $l(Q) \propto Q^{-1/3}$  is essentially the correlation length (2.24) in the mean field approximation. With these scalings the profiles are independent of  $Q$ .

and  $|\psi|$  vary substantially (Fig. 3), is expected to scale according to (2.24). We may estimate this width semi-quantitatively by defining a reduced temperature scale  $\epsilon_Q$  through equality in (3.2) and (3.3), and defining

$$\xi(Q) \equiv \xi(\epsilon_Q) \approx 24 \left( \frac{Q}{1 \mu\text{W}/\text{cm}^2} \right)^{-r\nu} \mu\text{m}, \quad r\nu \simeq 0.54. \quad (3.4)$$

The scaling relation (2.25) predicts  $r\nu = \nu_Q$  ( $= 1/2$  in  $d = 3$ ), requiring the scaling relation  $\mu = 1 - \zeta$  ( $\simeq 1/3$  in  $d = 3$ ) (Hohenberg and Halperin, 1977). The difference between experimental and theoretical values is presumably due to the quasi-scaling effect described at the end of Sec. II. Quantitative renormalization group based predictions for the full temperature profile  $T(z, Q)$ , explicitly including the quasi-scaling phenomenon (Haussmann and Dohm, 1991; Haussmann and Dohm, 1992a), are limited to the normal fluid region  $z < z_0$  where the vanishing of  $\psi$  greatly simplifies the calculations. Less quantitative predictions for the entire profile are limited to mean field (Onuki, 1983) (which ignores critical fluctuations) or large- $N$  (Haussmann, 1999a; Haussmann, 1999b) (which replaces the single complex order parameter with an  $N$ -component vector) approximations.

An experimental measurement of the temperature profile  $T(z, Q)$  within the interface region for a sequence of different  $Q$  would allow a detailed exploration of near-critical, nonlinear heat transport. It would also provide an experimental test of the scaling prediction (2.25). Such a measurement requires a regime in which  $\xi(Q)$  is larger than the width  $W$  of the thermometer. Present

technology places a limit  $W \gtrsim 50 \mu\text{m}$ . From (3.4), heat currents below  $1 \mu\text{W}/\text{cm}^2$  are required. Present technology allows controlled heat currents down to about  $1 \text{ nW}/\text{cm}^2$ , leading to  $\xi \approx 1 \text{ mm}$ , so at first sight such an experiment appears feasible.

In fact, Earth's gravity  $g_e$  places a fundamental limit on the maximum possible interface width. As described in Sec. I, gravity produces an equilibrium ( $Q = 0$ ) superfluid-normal fluid interface with width of order  $\xi(g_e) = 100 \mu\text{m}$ . From (3.4),  $\xi(Q) = \xi(g_e)$  for  $Q \simeq Q_g \equiv 70 \text{ nW}/\text{cm}^2$ . For  $Q$  of order  $Q_g$ , gravity will begin to have a strong effect on the nonequilibrium interface (Day *et al.*, 1998), and for  $Q \ll Q_g$  the heat current will be a small perturbation on the equilibrium interface. Thus  $\xi(Q)$  will saturate at  $\xi(g_e)$  as  $Q \rightarrow 0$  and the regime  $\xi(Q) \gg W$  is unattainable on Earth.

For this reason the critical dynamics experiment (DYNAMX) is currently being prepared for the microgravity environment of the International Space Station, with flight planned for 2004. Heat currents as low as  $5 \text{ nW}/\text{cm}^2$  will be used. The temperature profile  $T(z, Q)$  will be measured to subnanoKelvin resolution by slowly moving the interface past a fixed thermometer. The latter is accomplished by removing heat from the downstream end of the cell slightly more slowly than it enters the upstream end, with the effect that the normal phase slowly invades the cell, thus translating the interface.

## B. Transition from thermodynamic to interface state

We have discussed three possible classes of steady nonequilibrium states: (a) conducting normal states with static temperature profile determined by (3.1); (b) isothermal thermodynamic states with steady superfluid counterflow determined by (2.1); and (c) states with a nonequilibrium interface forming a “conversion boundary” between states of type (a) and (b). Transitions between (a) and (c) occur continuously: if state (a) is cooled to the point where the downstream endwall temperature passes through  $T_\lambda$ , an interface will form out of that endwall and steadily move upstream. Conversely, as heat is added to state (c), the interface will move downstream until the interface disappears into the endwall.

Similarly, the transition from (c) to (b) is continuous. The interface will disappear into the upstream endwall as heat is extracted, yielding an isothermal thermodynamic state at temperature  $T_\infty(Q)$ . Further extraction of heat will cause the temperature to drop below  $T_\infty(Q)$ .

The nature of the transition from (b) to (c) is less clear. At issue is whether the bulk superfluid, in the absence of an interface, recognizes  $T_\infty(Q)$  as a special temperature. Within the mean field approximation, the answer is no (Onuki, 1983): the thermodynamic state is stable up to a temperature  $T_c(Q)$ , with  $T_\lambda > T_c(Q) > T_\infty(Q)$ , whose

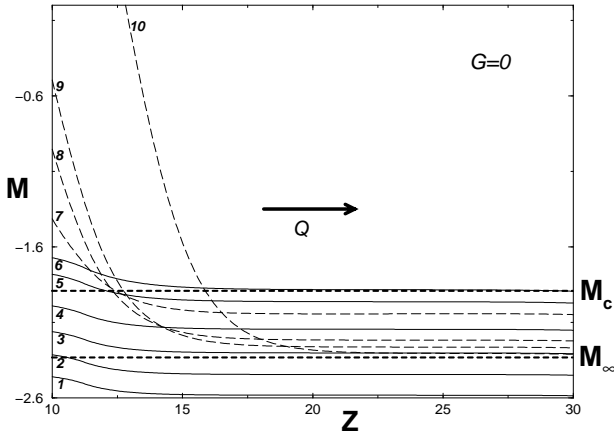


FIG. 4. For bulk scaled temperature  $M > M_c$  (see caption to Fig. 3) the uniform superfluid state becomes unstable to a state with an interface (Weichman and Miller, 2000). Curves 1-6 (solid) show consecutive *stable* (time independent) superfluid temperature profiles obtained in the mean field approximation upon slowly varying the right-hand wall temperature. Curves 7-10 show snapshots of the time evolution, computed within a simple one-dimensional model, initiated by a series of phase slips (not shown) after the right-hand wall temperature is raised slightly above that of curve 6. The key feature is the net temperature drop (from  $M_c$  to  $M_\infty$ ) observed in the bulk superfluid. Figure reprinted from (Weichman and Miller, 2000) courtesy of the Journal of Low Temperature Physics.

functional inverse  $Q_c(T)$  we might identify with the boundary in Fig. 1(b), at which the superfluid density is suppressed to the point where it is incapable of supporting the heat current. As shown in Fig. 4, when the thermodynamic state is heated above  $T_c(Q)$  a complicated dynamics results, with the system finally settling down into a state with an interface. Since  $T_\infty(Q) < T_c(Q)$ , the superfluid side actually *cools*, with a compensatory heating of the normal side. The final position of the interface is determined from energy conservation.

The question of whether or not a first order transition from (b) to (c) survives in some form beyond the mean field approximation is subtle, and is probably a question of time scale. The same thermal nucleation of vortices that leads to a small temperature gradient in the superfluid phase presumably also leads to a continuous (b) to (c) transition, with the interface entering continuously from the upstream endwall, if the experimental heating rate is infinitesimally slow. Any finite heating rate may, however, allow a “superheating” of (b), inducing an apparent first order transition to (c) nucleated by a random vortex creation event. Such an effect would be analogous to superheating and supercooling effects at conventional first order transitions, the boundary  $Q_c(T)$  being analogous to a spinodal line (defined roughly as the temperature at which a local free energy barrier separating the superheated or supercooled metastable state

from the true equilibrium state disappears, allowing rapid conversion to the thermodynamically stable phase).

Experimental investigation of the (b) to (c) transition is complicated by boundary effects. The singular Kapitza resistance leads to an additional heating of the upstream endwall, which then acts as a nucleation point for vortices even when the temperature of the bulk superfluid is still below  $T_\infty(Q)$  (Harter *et al.*, 2000). Clever cell designs that reduce the heat current near the endwall below that in the bulk may eventually allow experimental observation of a superheating effect.

### C. Interface dynamics

Despite the greatly reduced gravity, the Space Station environment is less than ideal for other reasons. Vibrational noise (“g-gitter”) exists at a level of about  $10^{-3}g_e$ , and one might worry that such noise might couple strongly to the interface, and perhaps destabilize it. Understanding the effects of acceleration noise requires an understanding of (a) the *free dynamics* of the interface when it is perturbed away from its steady state, e.g., whether or not the interface is even dynamically stable, or whether small perturbations might undergo some kind of “dendritic growth”, and (b) the manner in which vibration, or other perturbations, couple to, and perhaps amplify this motion (Weichman *et al.*, 1998).

Suppose that a slow variation,  $z_0 = z_0(\mathbf{r})$ , with the transverse coordinates  $\mathbf{r} = (x, y)$ , is applied to the interface position and is subsequently released. The problem is to derive an equation of motion for  $z_0(\mathbf{r}, t)$ . In order to motivate the interesting physical questions, it is useful to consider first the analogous problem of the motion of an *equilibrium* interface between up and down domains of an Ising ferromagnet, with diffusive “Model A” dynamics (Hohenberg and Halperin, 1977). *Surface tension* acts as a restoring force against perturbations away from a flat interface, and one may derive a *diffusion equation* for the relaxation of long wavelength perturbations of the interface position:

$$(\partial_t - D\nabla^2)z_0(\mathbf{r}, t) = \eta(\mathbf{r}, t), \quad (3.5)$$

in which the value of  $D$  depends on the microscopic parameters in the model, and the driving term  $\eta$ , vanishing for free relaxation, has been included for completeness. *Thermal fluctuations* in the spins lead to a Gaussian white noise form for  $\eta$  with correlator  $\langle \eta(\mathbf{r}, t)\eta(\mathbf{r}', t') \rangle = \zeta_0 \delta(\mathbf{r} - \mathbf{r}')\delta(t - t')$  where  $\zeta_0$  depends on microscopic parameters and on temperature. Using this form one may compute the equal time variance in the interface position

$$\begin{aligned} C(\mathbf{r} - \mathbf{r}') &\equiv \langle [z_0(\mathbf{r}, t) - z_0(\mathbf{r}', t)]^2 \rangle \\ &= \frac{\zeta_0}{4\pi D} \ln \left( \frac{|\mathbf{r} - \mathbf{r}'|}{a_0} \right), \end{aligned} \quad (3.6)$$



where  $a_0$  is an atomic length scale. One sees that fluctuations in the interface position *diverge* logarithmically with separation: a famous result known as *interface roughness*, encountered most frequently in discussions of crystal facet shapes. The interface is locally stable and flat, but globally wanders arbitrarily large distances.

The result (3.6) shows that there are subtle physical issues, lying beyond the much simpler question of stability, arising because the interface breaks the continuous translation invariance of the system. Whenever a continuous symmetry is broken, a Goldstone mode (namely, a slow dynamical mode arising when the local value of the broken symmetry varies slowly in space) is generated, corresponding in this case to very slow relaxation of long wavelength perturbations of the interface position,  $z_0 \propto e^{i\mathbf{k}\cdot\mathbf{r}-\lambda(\mathbf{k})t}$ , with (3.5) yielding  $\lambda = Dk^2$ . Such long wavelength “modes” are highly susceptible to thermal or externally generated noise spectrum  $\zeta(k)$ , and it is the convergence at small  $k$  of the integral

$$\langle z_0(\mathbf{r}, t)^2 \rangle = \int \frac{d^2k}{(2\pi)^2} \frac{\zeta(\mathbf{k})}{\text{Re}\lambda(\mathbf{k})}, \quad (3.7)$$

that determines whether or not the interface is rough. For the case  $\zeta(k) \equiv \zeta_0$ , (3.7) diverges logarithmically, which same divergence is reflected in the correlator (3.6).

The physics of the nonequilibrium superfluid-normal interface is very different from that of the equilibrium magnetic interface. As described, the dynamics of the latter is purely diffusive, with the two bulk phases on either side of it containing no slow dynamical modes of their own (since the order parameter is non-conserved and is not coupled to any other conserved field). In contrast, transport on the normal side of the  $^4\text{He}$  interface is controlled by slow heat diffusion, and transport on the superfluid side, controlled by superfluid counterflow, is essentially ballistic, and the dynamics of the interface itself therefore involves a very intricate coupling of *three* different slow dynamical modes: normal phase diffusion, superfluid phase counterflow, and the broken translational symmetry Goldstone mode of the interface itself. To leading order one finds an equation of motion (Weichman *et al.*, 1998)

$$(\partial_t^2 - c^2 \nabla^2) z_0(\mathbf{r}, t) = \eta(\mathbf{r}, t), \quad (3.8)$$

so that the interface supports *traveling wave* excitations, with a well defined speed  $c(Q)$  of the same order as the bulk second sound speed (the speed with which perturbations in the order parameter travel on the superfluid side of the interface). At next-to-leading order one finds that these excitations are *singularly damped*, with  $\lambda = ick + Dk^{3/2}$ , so that  $\text{Re}\lambda \propto k^{3/2}$  rather than  $k^2$  (as for bulk second sound waves) at small  $k$ . Positivity of  $\text{Re}D$  establishes intrinsic dynamical stability of the interface. One may interpret the enhanced damping as arising from

the waves on the interface “rubbing” up against the normal phase. Moreover, one finds that thermal fluctuations enter via a spectrum  $\zeta(k) \propto k^{5/2}$  for  $\eta$ , vanishing strongly as  $k \rightarrow 0$ . The physics of this result is related to the fact that interface motion is a *cooperative* phenomenon, involving evanescent dynamics of the superfluid order parameter to a depth  $\sim k^{-3/2}$  scaling as the  $3/2$  power of the wavelength.<sup>§</sup> The microscopic thermal noise, which is white, must then be averaged over a similar volume to obtain its net effect on the mode, leading eventually to the greatly reduced  $\zeta(k)$  above. In contrast, the Ising interface moves by local spin flips and the microscopic noise is averaged only over a microscopic region of width  $a_0$  and  $\zeta$  remains white.

The net result of the analysis is that the integral (3.7) is strongly convergent at  $k = 0$ , and the superfluid-normal interface is globally flat. This is good news for the Critical Dynamics Experiment (DYNAMX), where a rough interface would have led to substantial smearing of the temperature profile on a scale varying as the logarithm of the cell cross-section.

Vibrational acceleration noise couples to the interface in the same way that Earth’s gravity does, through the variation in the local  $T_\lambda$  with pressure. A slight change in  $T_\lambda$  will cause the interface to translate (for acceleration normal to the interface) or tilt (for acceleration parallel to the interface) slightly, but if the change is *oscillatory* it could resonate with one of the interfacial second sound modes, leading to a rapid growth in the interface motion. A detailed examination of the expected frequency spectrum of the Space Station g-gitter, together with the discrete spectrum of standing wave modes allowed in the experimental cell within the planned temperature and heat current range, shows that such resonances may indeed occur, but that the singular damping is sufficiently strong that the interface oscillation amplitude should saturate at acceptably low levels (Chui *et al.*, 1997).

The existence of the interfacial second sound mode has yet to be tested experimentally. This might be accomplished by applying a sequence of heat pulses to the cell sidewall near the interface and detecting a response at the opposite sidewall. Scattering of bulk second sound pulses off the interface, with detection of the reflected pulses, might also provide interesting information about the coupling of bulk and interface modes.

---

<sup>§</sup>The evanescent depth on the normal side is much smaller, scaling as  $k^{-1/2}$ . For comparison, gravity waves on fluid surfaces yield fluid motion to a depth  $\sim k^{-1}$  proportional to the wavelength.

#### IV. THE SELF-ORGANIZED CRITICAL STATE

We have so far discussed phenomena in which optimal conditions occur in the absence of gravity. It transpires that there is a very interesting phenomenon in which gravity and heat current *combine* to produce a new type of dynamical state. The so-called *self-organized critical* (SOC) state occurs in a cell which is heated from above, so that  $\mathbf{g}$  and  $\mathbf{Q}$  are parallel.\*\*

Gravity depresses the lambda point  $T_\lambda(z)$  with increasing depth according to (1.1), while heat current leads to decreasing temperature  $T(z)$  with depth according to (3.1). The reduced temperature  $\epsilon(z) \equiv [T(z) - T_\lambda(z)]/T_{\lambda,0}$ , where  $T_{\lambda,0}$  is, say, the bulk transition temperature if gravity were absent (and hence approximately the transition temperature at the top of the cell), contains a *competition* between these two effects. One might, in fact, imagine tuning  $Q$  in such a way that  $\epsilon(z)$  is independent of  $z$  (Onuki, 1987): the sample would apparently exist in an essentially homogeneous near-critical state. In fact, it was argued (Machta *et al.*, 1993; Ahlers and Liu, 1996) that the system actually “self-organizes”  $T(z)$  in order to enforce a uniform  $\epsilon$ . Assuming the validity of the Fourier law (3.1),  $\epsilon$  must be uniquely defined by

$$\kappa(\epsilon_{\text{SOC}}) = Q/|\partial_z T_\lambda|, \quad (4.1)$$

where  $\epsilon_{\text{SOC}}$ , a function of the ratio  $Q/g$ , is the reduced temperature of the new state. This state has recently been observed experimentally (Moeur *et al.*, 1997).

As an aside, we comment that the name SOC is motivated by similar self-tuning to a macroscopically homogeneous state under nonequilibrium conditions observed, for example, in “sandpile” models (Bak *et al.*, 1988), and in fluid turbulence. There, however, the self-organized state displays “avalanches” (vortical eddies in the fluid), with a power law distribution of sizes, analogous to similar power law-distributed fluctuations observed at equilibrium critical points, but without the requirement that an external parameter like temperature be tuned to obtain the critical state. Although the “SO” part of SOC is justified for the  $^4\text{He}$  state, the “C” part is not since analogous critical power laws have yet to be demonstrated either theoretically or experimentally, as should become clear below. The name, however, has stuck and we will not attempt to alter convention here.

The fact that  $\kappa$  increases with decreasing  $T$  ensures stability of the SOC state to small perturbations (Machta *et al.*, 1993; Ahlers and Liu, 1996). More specifically, an analysis of the heat diffusion equation in the normal

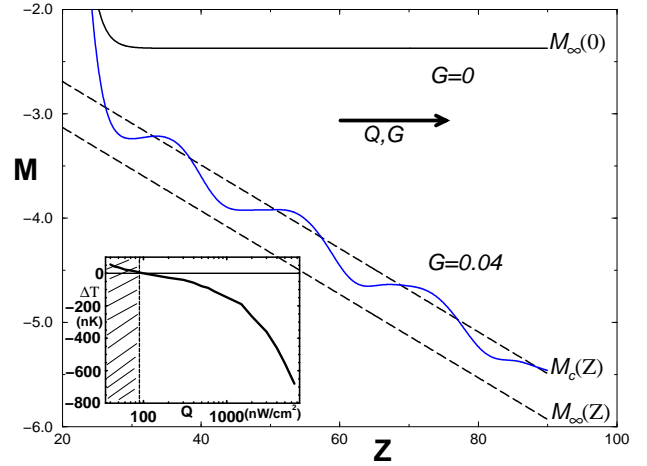


FIG. 5. Simulation of the SOC state using the same simplified 1-d model as in Fig. 4. For  $G \propto g/Q = 0$  the temperature gradient in the normal phase ( $Z \lesssim 20$ ) gives way to an asymptotically isothermal superfluid phase ( $Z \gtrsim 30$ ) with temperature  $T_\infty(Q) < T_{\lambda,0}$ . For  $G > 0$  the superfluid phase develops phase slips (vortices in 3-d), and a corresponding dynamic staircase structure in  $T(z)$ , roughly bounded between  $T_\infty(z)$  and  $T_c(z)$ , to produce the SOC state. The density of phase slips increases with  $G$ . Inset: experimental data replotted from Fig. 4 of (Moeur *et al.*, 1997) showing the self-organization temperature,  $\Delta T(Q) = T(Q, z) - T_\lambda(z)$ . Only for  $Q \lesssim 100 \text{ nW/cm}^2$  (small shaded region) is the SOC state in the normal phase. Figure reprinted from (Weichman and Miller, 2000) courtesy of the Journal of Low Temperature Physics.

phase (Weichman and Miller, 2000) shows that a perturbation  $\epsilon(\mathbf{x}) = \epsilon_{\text{SOC}} + \delta\epsilon(\mathbf{x})$  obeys an equation of motion whose solutions are decaying plane waves of the form

$$\delta\epsilon(\mathbf{x}, t) = \delta\epsilon(\mathbf{q}) e^{-D_{\text{SOC}} q^2 t} e^{i\mathbf{q} \cdot (\mathbf{x} + c_{\text{SOC}} \hat{\mathbf{z}} t)}, \quad (4.2)$$

with  $D_{\text{SOC}} = \kappa(\epsilon_{\text{SOC}})/C_p(\epsilon_{\text{SOC}})$  and  $c_{\text{SOC}} = -|\partial_z T_\lambda| \kappa'(\epsilon_{\text{SOC}})/T_{\lambda,0} C_p(\epsilon_{\text{SOC}})$ , where  $C_p$  is the equilibrium specific heat at constant pressure. Thus, in addition to the decay controlled by the diffusion constant  $D_{\text{SOC}}$ , there is an unexpected anisotropic propagation effect where the perturbation moves upstream at speed  $c_{\text{SOC}}$ . For the reasonable value  $Q = 50 \text{ nW/cm}^2$  (see below) one finds  $c_{\text{SOC}} \simeq 2.8 \text{ mm/s}$ , and the propagation effect should be experimentally observable for reasonable cell geometries (Weichman and Miller, 2000).

Since  $\kappa$  diverges as  $\epsilon \rightarrow 0$ , (4.1) implies that  $\epsilon_{\text{SOC}} \rightarrow 0$  as  $Q \rightarrow \infty$ . However, for large  $Q$  the Fourier law breaks down. In particular  $\kappa(T_\lambda, Q)$  is finite for  $Q > 0$  (Haussmann and Dohm, 1992a), and the SOC state must therefore lie below  $T_\lambda(z)$  for sufficiently large  $Q > Q_{\text{SOC}}$ . This is consistent with experimental data (Moeur *et al.*, 1997), reproduced in the inset to Fig. 5, which shows that  $\epsilon_{\text{SOC}} < 0$  for  $Q \gtrsim 100 \text{ nW/cm}^2$ . Using (4.1), along with (3.2) defining the validity of the Fourier law, one may show that the previous theory is valid for (Onuki,

\*\*When  $Q$  and  $g$  are antiparallel (heat from below) they cooperate to simply produce a sharper interface.

1996; Weichman and Miller, 2000)

$$6.1 \left( \frac{Q}{100 \text{ nW/cm}^2} \right)^{(1+\nu)/\mu} \left( \frac{g}{g_e} \right)^{1-(1+\nu)/\mu} \ll 1. \quad (4.3)$$

Equality in (4.3) serves an estimate for  $Q_{\text{SOC}}$  and yields  $Q_{\text{SOC}} \simeq 60 \text{ nW/cm}^2$  under Earth's gravity, in very reasonable agreement with the experimental result.

The question now remains as to the nature of the SOC state below  $T_\lambda$ . The state must undergo some kind of transition to superfluidity, but the fact that it continues to support a finite temperature gradient appears inconsistent with the isothermal nature of a superfluid. The resolution of this paradox is shown in Fig. 5. Let  $T_\infty(z) = T_\lambda(z) - \Delta T_\infty(Q)$  and  $T_c(z) = T_\lambda(z) - \Delta T_c(Q)$  define local values of the interface and instability temperatures discussed in Sec. III.B, where  $\Delta T_c = T_{\lambda,0} - T_c(Q)$  and  $\Delta T_\infty = T_{\lambda,0} - T_\infty(Q)$  are the deviations from  $T_\lambda$  in zero gravity. For  $g = 0$  an interface state, represented by the upper curve in Fig. 5, is formed. For  $g > 0$ ,  $T(z)$  first drops below the local transition at a point  $z_0$ , and attempts to asymptote to an isothermal superfluid at a temperature close to  $T_\infty(z_0)$ . However, at a point  $z_1 > z_0$ , the descending line  $T_c(z_1)$  meets  $T_\infty(z_0)$  and the superfluid becomes unstable. A vortex is generated and crosses the cell, leading to dissipation and a finite temperature drop across it. By this mechanism the temperature is able to drop below the instability temperature and asymptote once again to an isothermal superfluid at a temperature close to  $T_\infty(z_1)$ . The entire scenario then repeats itself approximately periodically at a sequence of points  $z_n$ ,  $n = 1, 2, 3, \dots$ , where  $T_c(z_n)$  meets  $T_\infty(z_{n-1})$ . The result is a dynamic staircase structure, a snapshot of which is represented by the lower curve in Fig. 5. This structure fluctuates in time as vortices form and annihilate, but is found numerically to slowly move in an escalator-like fashion upstream (Weichman and Miller, 2000).

The time resolution of present thermometry is far too poor to detect fluctuations in the temperature profile, whose mean would correspond to a straight line parallel to and somewhere between  $T_\infty(z)$  and  $T_c(z)$ .<sup>††</sup> Experiments to detect the predicted stream of vortices, via the noise they emit in the form of second sound, are in the planning stages. Note that only if further numerical or experimental investigation were to reveal power law spatial and/or temporal correlations in the vortex nucleation events (as exhibited, for example, in  $1/f$ -type second sound noise spectra) would one obtain *a posteriori* evidence in support of the “C” in SOC.

<sup>††</sup>A renormalization group calculation of this mean profile as a function of  $Q$  in the large- $N$  limit is described in (Haussmann, 1999a; Haussmann, 1999b).

A simple calculation shows that the distances between vortices must scale as  $z_n - z_{n-1} \approx [\Delta T_\infty(Q) - \Delta T_c(Q)]g_e/\gamma g$ , increasing with larger  $Q$  and smaller  $g$ . Although the SOC state requires finite gravity, the regime of widely separated vortices may in the future prove sufficiently interesting that a controlled low gravity experiment will become desirable.

## V. SPECIFIC HEAT AT CONSTANT HEAT CURRENT

### A. Enhanced specific heat

The presence of a heat current is predicted to enhance the specific heat of superfluid  $^4\text{He}$  above its equilibrium value,  $C_0$ . This can easily be seen at low  $Q$ , sufficiently far below  $T_\lambda$ , where the free energy enhancements are  $\Delta F(T, \mathbf{U}_s) = \frac{1}{2}\rho_s \mathbf{U}_s^2$  and  $\Delta \Phi(T, \mathbf{J}_s) = -\mathbf{J}_s^2/2\rho_s$ , in which  $\rho_s(T) \approx \rho_0|\epsilon|^\zeta$  is the equilibrium superfluid density. Thus, at fixed superfluid velocity  $\mathbf{U}_s$ ,

$$\Delta C_{U_s} \equiv C_{U_s} - C_0 \approx T\rho_s \mathbf{U}_s^2 \zeta(1 - \zeta)/2T_\lambda^2|\epsilon|^2 > 0, \quad (5.1)$$

while at fixed heat current  $\mathbf{Q}$ ,

$$\Delta C_Q \equiv C_Q - C_0 \approx T\mathbf{J}_s^2 \zeta(1 + \zeta)/2T_\lambda^2\rho_s|\epsilon|^2 > 0. \quad (5.2)$$

Closer to  $T_\lambda$  the superfluid density depends strongly on heat current and the apparent divergences at  $T_\lambda$  in (5.1) and (5.2) are replaced by new singularities at the phase boundary  $T_c(U_s)$  shown in Fig. 1(b). It is predicted that  $\Delta C_{U_s}$  will remain finite, rising to a cusp at the phase boundary (Haussmann and Dohm, 1994), while  $\Delta C_Q$  is predicted to diverge (Chui *et al.*, 1996; Haussmann and Dohm, 1996). The latter result follows on very general grounds from the thermodynamic conjugacy of  $\mathbf{U}_s$  and  $\mathbf{J}_s$  discussed in Sec. II. The usual thermodynamic manipulations imply the relation

$$C_Q = C_{U_s} + T \left( \frac{\partial \mathbf{J}_s}{\partial T} \right)_{U_s}^2 \left( \frac{\partial U_s}{\partial \mathbf{J}_s} \right)_T. \quad (5.3)$$

Since the susceptibility,  $(\partial U_s/\partial \mathbf{J}_s)_T$  [proportional to the slope of the curve in Fig. 2(b)] is expected to diverge at the phase boundary, while  $(\partial \mathbf{J}_s/\partial T)_{U_s} = U_s(\partial \rho_s/\partial T)_{U_s}$  remains finite,  $C_Q$  will exhibit a *divergent* enhancement.

There have been no measurements of  $C_{U_s}$  to date, but an experiment of this kind might be performed in the presence of a persistent current flowing around a loop, similar to the superfluid gyroscope experiment (Clow and Reppy, 1972), where in the absence of vortices  $\mathbf{U}_s$  indeed remains fixed as  $T$  is varied. A measurement could prove difficult due to the small magnitude of the enhancement and the challenge of holding  $\mathbf{U}_s$  constant while measuring the specific heat. However, it has been suggested that with very fast thermometry, a measurement of  $C_{U_s}$  might be obtained through a second-sound measurement where

the second-sound waves are propagated perpendicular to  $\mathbf{U}_s$  (Haussmann, 1997).

Measurement of  $C_Q$  is more straightforward. The predicted divergence of  $\Delta C_Q$ , together with the fact that  $\mathbf{Q}$  can be experimentally controlled with great precision, implies a much more visible experimental signature. The first experimental measurements of this quantity were recently reported (Harter *et al.*, 2000). As will be discussed below, they indicate that the heat capacity is indeed enhanced, but with a magnitude that is significantly larger than theoretical predictions.

## B. The superfluid breakdown temperature

Experiments performed at constant  $Q$  should find that  $C_Q$  diverges at a temperature  $T_c(Q) < T_\lambda$ , defined by inverting (2.20):

$$|\epsilon_c(Q)| = \frac{T_\lambda - T_c(Q)}{T_\lambda} = \left( \frac{Q}{Q_0^c} \right)^x, \quad (5.4)$$

where  $Q_0^c = Q_0 y_c$  and  $x = 1/\Delta_Q = 1/2\nu \simeq 0.746$  (Onuki, 1984; Haussmann and Dohm, 1991; Goodstein *et al.*, 1996). Based on a renormalization group analysis of the Model F equations (Hohenberg and Halperin, 1977), in an approximation neglecting vortices (and hence decay of superflow), the prediction  $Q_0^c \approx 7.4 \text{ kW/cm}^2$  was obtained (Haussmann and Dohm, 1992b). More recently, using an extension of this theory, accounting for dissipation within a large- $N$  approximation, the value  $Q_0^c \approx 6.6 \text{ kW/cm}^2$  was obtained (Haussmann, 1999b).

These theoretical results disagree with the results of thermal conductivity experiments (Duncan *et al.*, 1988). The onset of thermal resistance was found to occur at a temperature which we call  $T_{\text{DAS}}(Q)$  that obeys (5.4), but with  $x = 0.813 \pm 0.012$  and  $Q_0^c = 568 \pm 200 \text{ W/cm}^2$ . This is a curve in the  $T$ - $Q$  plane that falls below the theoretically estimated  $T_c(Q)$  for all experimentally accessible temperatures (see Fig. 6). A number of explanations have been proposed for the discrepancy: (a) the transition at  $T_{\text{DAS}}(Q)$  may be caused by a temperature instability at the cell wall associated with the singular Kapitza resistance [which raises the temperature near the bottom (heated) end plate above that of the bulk, which therefore could serve as a vortex nucleation center], and hence lies below  $T_c(Q)$  (Harter *et al.*, 2000); (b)  $T_{\text{DAS}}$  may be related to a gravity-dependent transition, again lying below  $T_c(Q)$ , and will increase towards  $T_c(Q)$  as gravity is reduced, e.g., by going into space (Haussmann, 1999b); (c) since the transition is only sharply defined in the absence of vortices,  $T_{\text{DAS}}(Q)$  might be analogous to a spinodal line in a first-order phase transition (Liu and Ahlers, 1996): fluctuation-induced vortices nucleate the transition to the dissipative phase, and  $T_{\text{DAS}}(Q)$  will differ from experiment to experiment, depending on the heating rate

used. Since any superfluid state above  $T_\infty(Q)$  should be unstable by this mechanism, an infinitesimally slow experiment should find the transition at  $T_\infty(Q)$ .

It is possible that all of these effects (and perhaps others) are present. The real question, whose resolution clearly requires more experimental data, is which one imposes the most severe limitation on present experiments. The answer to this question has implications for the measurement of  $C_Q(T)$ . If effect (c) is dominant, then experiments have basically already reached the intrinsic limit on how close they can approach the divergence of  $C_Q(T)$  (for the range of  $Q$  explored thus far), though it may be possible to design an experiment with faster heating rates and fast enough thermometers to reach  $T_c(Q)$  before a vortex can nucleate. On the other hand, if proposal (b) is correct, a space-based microgravity measurement of  $C_Q(T)$  should be able to get considerably closer to  $T_c(Q)$  than one performed on the ground. If proposal (a) is correct, carefully designed ground-based experiments might be able to approach  $T_c(Q)$  more closely: if  $T_{\text{DAS}}$  is due to a boundary effect, a cell constructed with a bottom plate that is much larger than the cross-sectional area of the bulk helium sample could decrease the singular Kapitza resistance sufficiently so that the bulk helium can reach  $T_c(Q)$  without a boundary instability interfering. A cell of this configuration that maintains a reasonable geometry for heat flow would have to be fairly tall and might therefore be more susceptible to gravity effects.

## C. Experimental measurements

The first experimental measurements of  $C_Q(T)$  (Harter *et al.*, 2000) confirm the predicted enhancement, but find that its magnitude is significantly larger than current predictions (Chui *et al.*, 1996; Haussmann and Dohm, 1996; Haussmann, 1999b). The data were taken over the range  $1 \mu\text{W/cm}^2 \leq Q \leq 4 \mu\text{W/cm}^2$ , and a representative set at  $Q = 3.5 \mu\text{W/cm}^2$  is shown in Fig. 7.

The extent of the disagreement between theory and experiment can be observed more clearly when the data are plotted in scaled form. All theories predict that the enhancement should obey a scaling form

$$\Delta C_Q = |\epsilon|^{-\alpha} f_{J_s} \left[ \frac{Q}{Q_c(T)} \right], \quad (5.5)$$

where  $f_{J_s}(x)$  is a universal scaling function. From (5.2) and the scaling relations in Table I, for  $x \ll 1$  one has

$$f_{J_s}(x) = f_2 x^2 + O(x^4) \\ f_2 \equiv [\zeta(\zeta + 1)(Q_0^c)^2 / 2\rho_0 T_\lambda^3 S_\lambda^2]. \quad (5.6)$$

Using the theoretical estimates one obtains  $f_2 = 8.9 \text{ J/mol K}$  for  $Q_0^c = 7.4 \text{ kW/cm}^2$  and  $f_2 = 7.0 \text{ J/mol K}$  for  $Q_0^c = 6.6 \text{ kW/cm}^2$ , where the molar volume  $27.38 \text{ cm}^3/\text{mol}$  has been used to obtain familiar units.

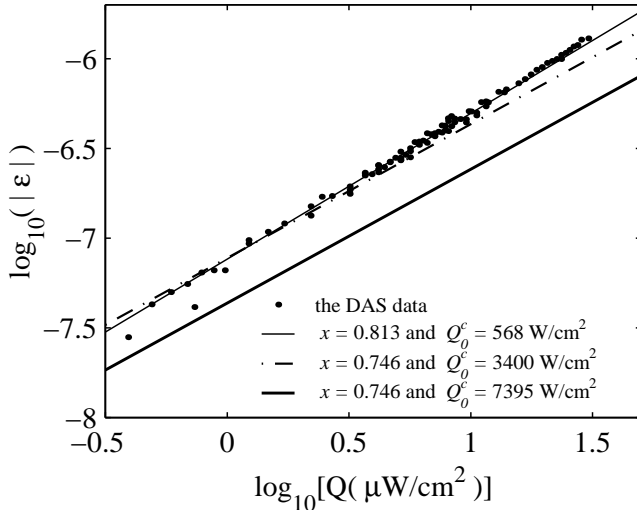


FIG. 6. Thick solid line:  $T_c(Q)$ , the theoretically predicted temperature of superfluid breakdown (Haussmann and Dohm, 1992b). Thin solid line:  $T_{\text{DAS}}(Q)$ , where the exponent  $x$  and amplitude  $Q_0^c$  are chosen to best fit to the observed temperature of superfluid breakdown represented by the data points (Duncan *et al.*, 1988). Dashed-dotted line: the value of  $Q_0^c$  that, along with the theoretical value  $x = 1/2\nu$ , makes the experimental heat capacity data match the more recent theoretical prediction for the scaling function (Haussmann, 1999b) (see Fig. 9 below).

In Fig. 8 we show the heat capacity enhancement as a function of the scaling variable  $(Q/Q_c)^2$ . Since  $Q_c(T)$  is not actually measured in the experiment, we scale the data using the theoretically predicted form  $Q_c = Q_0^c |\epsilon|^{\Delta_Q}$  with  $Q_0^c = 6.6 \text{ kW/cm}^2$  and  $\Delta_Q = 2\nu = 1.342$  (Haussmann, 1999b). As anticipated, the data for all  $Q \geq 2 \text{ } \mu\text{W/cm}^2$  collapse onto a single linear curve, verifying that the exponent  $\Delta_Q$  is at least consistent with the data. However, the slope of the experimental line is  $f_2^{\text{expt}} = 69 \pm 4 \text{ J/mol K}$ , approximately ten times larger than the theoretical prediction.

An optimistic explanation for the discrepancy between theory and experiment is that the theories are producing reasonable estimates for the universal scaling function  $f_{J_s}(x)$ , but that the nonuniversal amplitude  $Q_0^c$ , depending on detailed properties of the  $^4\text{He}$  system and therefore more difficult to compute, is estimated less accurately. As illustrated in Fig. 9(a), the choice  $Q_0^c = 3.4 \text{ kW/cm}^2$ †† in fact places the experimental data on top of the more recent theoretical curve (Haussmann, 1999b). With this

††This value is in fact within the estimated margin of error for the amplitude calculation. The uncertainty of the theory is a factor  $< 2$  (R. Haussmann, private communication), while the adjustment here is  $\simeq 1.9$ .

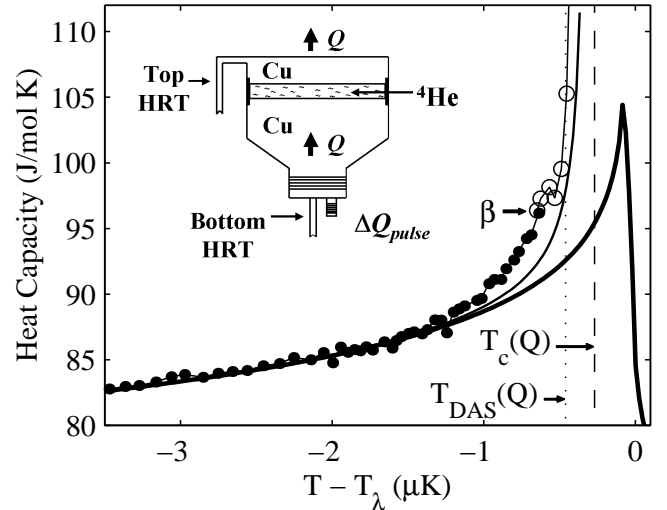


FIG. 7. Sample heat capacity data for  $Q = 3.5 \text{ } \mu\text{W/cm}^2$  (Harter *et al.*, 2000). Thick solid line: equilibrium  $C_0$  obtained from a fit to the Lambda Point Experiment (LPE) data (Lipa *et al.*, 1996) that is subsequently rounded for gravity. Thin solid line: theoretical prediction (Haussmann, 1999b) that includes vortices (rounded for gravity). Solid circles: data from the average of the top and bottom thermometers. Open circles: data from the top thermometer only [beyond the point marked  $\beta$ , where the bottom (hotter) thermometer was found to change its behavior, perhaps as a result of a boundary heating effect]. The temperature  $T_{\text{DAS}}$  marks the onset of dissipation found in earlier thermal conductivity experiments (Duncan *et al.*, 1988), while  $T_c(Q)$  is estimated from a certain theoretical fit to the data discussed later in the text. Inset: schematic diagram of the experimental cell. HRT stands for high resolution thermometer.

choice,  $T_c(Q)$  lies somewhat above  $T_{\text{DAS}}(Q)$  (vertical dashed line in Fig. 6). A somewhat smaller choice for  $Q_0^c$  would provide an equally good fit to the earlier theory (Haussmann and Dohm, 1992b). Unfortunately, all of the data lie at fairly small  $(Q/Q_c)^2 \leq 0.3$  where the scaling function has little structure (essentially indistinguishable from linear within the scatter of the data). A true test would require data in the regime  $(Q/Q_c)^2 \rightarrow 1$  where the scaling function diverges.

For completeness we also show in Fig. 9(b) an equally good scaling collapse based on the assumption that  $T_c(Q) \approx T_{\text{DAS}}(Q)$ . Thus, we use  $Q_c(T)$  derived from (5.4) using  $x = 0.813$  (i.e., effectively  $\nu = 0.615$ ) and  $Q_0^c = 0.65 \text{ kW/cm}^2$  [optimally chosen within the error bars quoted in (Duncan *et al.*, 1988)]. Since  $T_{\text{DAS}}$  places a lower bound on  $T_c(Q)$ , the sharpest conclusion we can make at this stage is that the data are consistent with the scaling hypothesis for a fairly broad range of experimentally and theoretically motivated parameter choices and that more data closer to  $T_c(Q)$  will be required for a critical test of the theory.

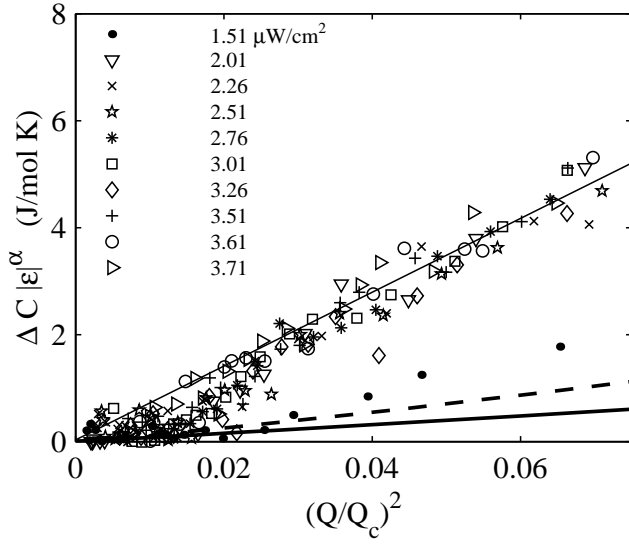


FIG. 8. Scaling plot of the differential heat capacity measurements for various values of  $Q$  (Harter *et al.*, 2000). The experimental data are scaled using  $Q_0^c = 6.6 \text{ kW/cm}^2$ , and terminated at the temperature indicated by  $\beta$  in Fig. 7. The predicted collapse of the data for different  $Q$  values onto nearly the same curve verifies the basic scaling hypothesis (5.5). Thin solid line: straight line fit to the data. Thick solid line: theoretical prediction neglecting dissipation (Chui *et al.*, 1996; Haussmann and Dohm, 1996). Dashed line: theoretical prediction including dissipation (Haussmann, 1999b). Neither theoretical curve is rounded for gravity.

The experimental measurements were taken in a cell that was only 0.64 mm high, about as close to the optimal height as practical considerations allow. Although the effects of gravitational rounding were therefore minimized, they were not entirely eliminated. The variation of  $T_\lambda$  across the cell due to gravity was  $\delta T_\lambda \simeq 8 \times 10^{-8} \text{ K}$ . A reasonable criterion for a data point to be unaffected by gravity is that one should have  $|T - T_\lambda| \geq 10\delta T_\lambda$ . This would restrict the temperature range of the experiment to more than about  $1 \mu\text{K}$  below  $T_\lambda$ . Essentially none of the interesting data shown in Figs. 7–9 satisfy this criterion. In fact, because measurements (Baddar *et al.*, 1999) have shown that under a heat flux  $Q > 4 \mu\text{W/cm}^2$ , helium exhibits appreciable dissipation, there is no range of parameters for which this criterion can be satisfied under Earth’s gravity in an isothermal experiment that measures  $C_Q$  close to  $T_c(Q)$ .

The small cell height used in the experiment precluded the use of side-wall thermometry. The helium temperature was measured using thermometers mounted on the cell end-plates and the data were corrected for the singular Kapitza resistance (Fu *et al.*, 1998). The temperature range of the measurements was limited because the bottom (hotter) thermometer changed its behavior before the bulk helium temperature reached  $T_{DAS}(Q)$  (Harter

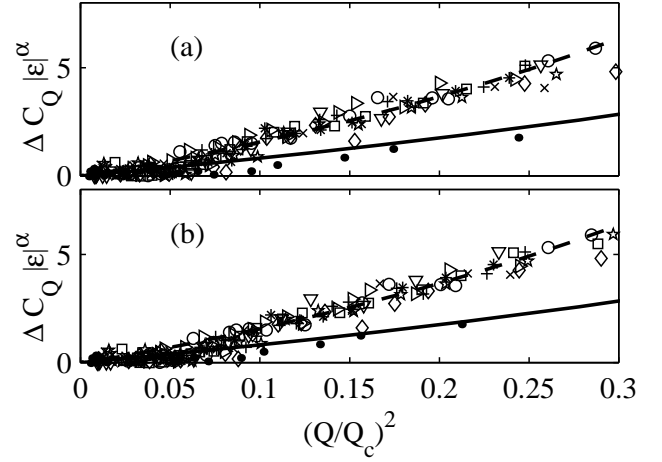


FIG. 9. Alternative scaling plot of the differential heat capacity measurements for various values of  $Q$  (Harter *et al.*, 2000). The data symbols are the same as those used in Fig. 8. The experimental data are scaled using  $Q_c(T)$  derived from (5.4) by (a) using the theoretical exponent value  $x = 1/2\nu = 0.746$ , but amplitude  $Q_0^c = 3.4 \text{ kW/cm}^2$  chosen to best match the theoretical scaling function; and by (b) assuming that  $T_c(Q) \approx T_{DAS}(Q)$  with  $Q_0^c = 0.65 \text{ W/cm}^2$  and  $x = 0.813$ . For the  $Q$ -range of the experimental data, the two analyses are basically identical, with the lines completely overlapping to well within experimental resolution. Only for higher  $Q$  data would the two fits become distinguishable. Solid line: theoretical prediction neglecting dissipation (Chui *et al.*, 1996; Haussmann and Dohm, 1996); Dashed line: theoretical prediction including dissipation (Haussmann, 1999b).

*et al.*, 2000). It was proposed that this change was due to another boundary effect related to the Kapitza resistance. The temperature at which this phenomenon occurred is indicated by  $\beta$  in Fig. 7, and is the maximum temperature of the data shown in Figs. 8 and 9. As a result of the reduced range, the data in Fig. 9 do not reach high enough temperatures to encounter much curvature in the scaling function. Measurements that approach closer to the divergence are clearly needed. Data up to  $T_{DAS}(Q)$  should be easily obtainable using a deeper cell constructed with a mid-plane thermometer. However, since rounding due to gravity will be even more of a detriment over the region where the scaling function has significant curvature, the ill-effects of the deeper cell height will obscure some of the benefit gained by the increased temperature range.

The only definitive way to circumvent the problems raised in the previous two paragraphs is to perform a space-based measurement of  $C_Q$ . An experiment in the absence of gravity would obtain data up to  $T_{DAS}(Q)$  without gravitational rounding, permitting an extension of the scaling data into a more revealing temperature range. This would allow a considerably improved estimate of where  $T_c(Q)$  lies in relation to  $T_{DAS}(Q)$  [in

particular if  $\Delta C_Q$  is still finite at  $T_{\text{DAS}}(Q)$  one would conclude that  $T_c(Q) > T_{\text{DAS}}(Q)$ . Furthermore, a space experiment would test the suggestion that  $T_{\text{DAS}}(Q)$  is a gravity artifact (Hausmann, 1999b), and permit the construction of a deep cell with asymmetric endplates to test whether  $T_{\text{DAS}}(Q)$  is a boundary effect.

## VI. CONCLUSIONS

We have reviewed the current status of experiment and theory of liquid helium when it is very close to the superfluid transition, but not in equilibrium. Nonequilibrium states are most easily probed experimentally by passing a uniform heat flux,  $\mathbf{Q}$ , through the liquid. If the average temperature of the sample is sufficiently far above  $T_\lambda$ , the heat flux produces a uniform temperature gradient, given by (3.1). Below  $T_\lambda$ , a sufficiently small  $Q$  produces a uniform temperature. Between these limits there is a nonlinear regime that is only partially understood.

In the uniform temperature regime below  $T_\lambda$ ,  $\mathbf{J}_s$  (proportional to  $\mathbf{Q}$ ) and  $\mathbf{U}_s$  may be treated as conjugate thermodynamic variables [see (2.4)]. By analogy to equilibrium critical point phase transitions, one can imagine a critical region in the  $Q$ - $T$  plane, and we are able to define new critical point exponents for these conjugate variables, and derive scaling laws between them that permit all of them to be evaluated in the critical region. These predictions have undergone only limited experimental tests.

In all instances, the nature of the nonequilibrium phase transition is strongly affected by gravity. If the heat flux is in the opposite direction to gravity, the transition can be made to occur within the cell, the bottom end where the heat enters being normal, and the top, where the heat is removed, superfluid. In this case, the width of the interface, which is the nonlinear region, is dominated by Earth's gravity at the very low values of  $Q$  that are of primary interest to investigations of critical phenomena, and is too small to be probed experimentally. If the heat flux is in the same direction as gravity, the system develops a temperature gradient equal to the gravity induced gradient in  $T_\lambda$ , so that it has the same reduced temperature everywhere. This is the so-called SOC state. At small  $Q$ , the SOC state can be on the normal side of the transition. At larger  $Q$  it exists on the superfluid side, the temperature gradient being maintained by a dynamic mechanism of vortex production.

On the superfluid side of the transition, the heat capacity,  $C_Q$ , is expected to be larger than  $C_Q(Q=0)$ , and in fact to diverge at the phase boundary. Preliminary experiments show that  $C_Q$  is indeed enhanced, and in fact is far larger than expected theoretically. It is not known whether this discrepancy is due to uncertainty in the position of the phase boundary or to other causes.

This result too is strongly affected by gravity, which introduces an inhomogeneity in the reduced temperature,  $\epsilon$ , at the small values of  $\epsilon$  necessary for these experiments.

Although much progress has been made in understanding this nonequilibrium phase transition and exploring the exciting new physics that it exhibits, it is clear that experiments in the absence of Earth's gravity will be needed. One such experiment (DYNAMX) is in preparation, and others are planned.

## REFERENCES

- Ahlers, G., and F.-C. Liu, 1996, J. Low Temp. Phys. **105**, 255.
- Baddar, H., G. Ahlers, K. Kuehn, and H. Fu, 1999, preprint.
- Bak, P., C. Tang and K. Wiesenfeld, 1988, Phys. Rev. A **38**, 364.
- Chui, T. C. P., D. L. Goodstein, A. W. Harter and R. Mukhopadhyay, 1996, Phys. Rev. Lett. **77**, 1793.
- Chui, T. C. P., P. B. Weichman, R. Galletly, D. Elliott, K. Aaron and D. L. Goodstein, 1997, *DYNAMX vibration requirement*, DYNAMX Design File #27 (DX-DF-27).
- Clow, J. R., J. D. Reppy, 1972, Phys. Rev. A **5** 424.
- Day, P. K., W. A. Moeur, S. S. McCready, D. A. Sergatskov, F.-C. Liu and R. V. Duncan, 1998, Phys. Rev. Lett. **81**, 2474.
- Dingus, M., F. Zhong and H. Meyer, 1986, J. Low Temp. Phys. **65**, 185.
- Dohm, V., 1991, Phys. Rev. B **44**, 2697 (1991).
- Duncan, R. V., G. Ahlers and V. Steinberg, 1988, Phys. Rev. Lett. **60**, 1522.
- Duncan, R. V. and G. Ahlers, 1991, Phys. Rev. B **43**, 7707.
- Fisher, M. E., 1973, Proc. Nobel Symp. **24**, 16.
- Fisher, M. E., 1983, *Scaling, universality and renormalization group theory* in Critical Phenomena, Lecture Notes in Physics (Springer-Verlag, Berlin), **186**, 1, F. J. W. Hahn, editor.
- Fu, H., H. Baddar, K. Kuehn, and G. Ahlers, 1998, Low Temp. Phys. **24**, 69.
- Giordano, N., P. Muzikar, and S. S. C. Burnett, 1987, Phys. Rev. B **36**, 667.
- Goldner, L., and G. Ahlers, 1992, Phys. Rev. B **45**, 13129.
- Goodstein, D. L., T. C. P. Chui, and A. W. Harter, 1996, Phys. Rev. Lett. **77**, 979.
- Greywall, D.S., and G. Ahlers, 1973, Phys. Rev. A **7**, 2145.
- Harter, A. W., R. A. M. Lee, A. Chatto, X. Wu, T. C. P. Chui and D. L. Goodstein, 2000, Phys. Rev. Lett. **84**, 2195.
- Hausmann, R., 1997, J. Low Temp. Phys. **107**, 21.
- Hausmann, R., 1999a, J. Low Temp. Phys. **114**, 1.
- Hausmann, R., 1999b, Phys. Rev. B **60**, 12349.
- Hausmann, R., and V. Dohm, 1991, Phys. Rev. Lett. **67**, 3404.
- Hausmann, R., and V. Dohm, 1992a, Z. Phys. B **87**, 229.
- Hausmann, R., and V. Dohm, 1992b, Phys. Rev. B **46**, 46.
- Hausmann, R., and V. Dohm, 1994, Phys. Rev. Lett. **72**, 3060.
- Hausmann, R., and V. Dohm, 1996, Czech. J. Phys. **46-S1**,

- 171.
- Hohenberg, P. C., A. Aharony, B. I. Halperin and E. D. Siggia, 1976, Phys. Rev. B **13**, 2986.
- Hohenberg, P. C., and B. I. Halperin, 1977, Rev. Mod. Phys. **49**, 435.
- Hohenberg, P. C., and P. C. Martin, 1965, Ann. Phys. (N.Y.) **34**, 291.
- Landau, L.D. 1941, USSR **5**, 71. [English translation: 1965, *Collected Papers of L.D. Landau*, D. ter Haar, editor, (Gordon and Breach, New York), p. 301.]
- Langer, J. A., and M. E. Fisher, 1960, Phys. Rev. Lett. **19**, 560 (1960).
- Lipa, J. A., D. R. Swansson, J. A. Nissen, T. C. P. Chui and U. E. Israelson, 1996, Phys. Rev. Lett. **76**, 944.
- Liu, F.-C., and G. Ahlers, 1996, Phys. Rev. Lett. **76**, 1300.
- Machta, J., D. Candela, and R. B. Hallock, 1993, Phys. Rev. B **47**, 4581.
- Moeur, W. A., P. K. Day, F.-C. Liu, S. T. P. Boyd, M. J. Adriaans, and R. V. Duncan, 1997, Phys. Rev. Lett. **78**, 2421.
- Muzikar, P., and N. Giordano, 1989, Physica A **157**, 742.
- Onuki, A., 1983, J. Low Temp. Phys. **50**, 433.
- Onuki, A., 1984, J. Low Temp. Phys. **55**, 309.
- Onuki, A., 1987, Jpn. J. Appl. Phys. **26**, 365.
- Onuki, A., 1996, J. Low Temp. Phys. **104**, 133.
- Onuki, A., and Y. Yamazaki, 1996, J. Low Temp. Phys. **103**, 131.
- Pfeuty, P., D. Jasnow and M. E. Fisher, 1974, Phys. Rev. B **10**, 2088.
- Tam, W. Y., and G. Ahlers, 1985, Phys. Rev. B **32**, 5932; **33**, 183 (1986).
- Weichman, P. B., and J. Miller, 2000, J. Low Temp. Phys. **119**, 155.
- Weichman, P. B., A. Prasad, R. Mukhopadhyay and J. Miller, 1998, Phys. Rev. Lett. **80**, 4923.